SYNTHESIS OF MICROWAVE-ASSISTED RISE HUSK BASED ACTIVATED CARBON FOR ADSORPTION OF METHYLENE BLUE DYE

Erniza Mohd Johan Jaya[1], Mohamad Firdaus Mohamad Yusop[1], Muhammad Nasri Nasehir Khan[1], Iylia Idris[2] and Mohd Azmier Ahmad[1,*]

[1]School of Chemical Engineering, Engineering Campus, Universiti Sains Malaysia,
14300 Nibong Tebal, Pulau Pinang, Malaysia.
[2]School of Chemical Engineering, College of Engineering, Universiti Teknologi MARA,
40450 Shah Alam, Selangor, Malaysia.

*chazmier@usm.my

Abstract. This research attempts to remove extremely toxic methylene blue dye (MB) from water through adsorption process using rice husk based activated carbon (RHAC). This work utilized a simple RHAC preparation method from rice husk via microwace irridiation activation process involving carbon dioxide, CO_2 gasification. Response surface methodology (RSM) was implemented to obtained an optimum preparation conditions of RHAC. The optimum preparation conditions were at microwave radiation power of 440 W for 4.28 minutes of activation time, which gave 83.93 % of MB removal and RHAC yield of 32.55 %. Adsorption performance of RHAC for MB removal was evaluated by batch adsorption process where the effects of 3 different variables (initial MB concentration, contact time and solution temperature) were studied. As MB initial concentration increased, the MB uptakes increased whilst MB percentage removal decreased. MB uptakes and percentage removal were found to increase with contact time. Highest MB removal was obtained at highest solution temperature of 60 °C with 88.82 %, thus signified endothermic nature. Characterization results showed an improvement in terms of surface functionality (Fourier-transform infrared spectroscopy, FTIR), high fixed carbon content of 70.34 %, and excellent physical properties where optimized RHAC have pore volume of 0.35 cm^3/g, surface area of 668.30 m^2/g and average pore diameter of 4.42 nm. Last but not least, the adsorption equilibrium analysis of RHAC/MB adsorption system was found to well matched the Freundlich isotherm. Meanwhile, for adsorption kinetic analysis, pseudo-first-order kinetic model was best suited the MB-RHAC system.

Keywords: Adsorption, activated carbon, optimization, RSM, dye

---

Article Info

Received 6th March 2023
Accepted 29th April 2023
Published 1st May 2023

ISSN: 1823-7010, eISSN: 2600-7444

Introduction

Methylene blue (MB) is an in demand synthetic dyes that vastly utilized in various industries such as beauty industry, leather, paper, pharmaceutical, food, and most commonly, textile industry. As a matter of fact, textile industry is deemed as the most waters polluted industry due to high usage of synthetic dyes and large amount of water consumed in dyeing process that contributes to the huge volume of wastewater production. Methylene blue dye is categorized as a noxious colorant with carcinogenic and mutagenic properties. The complex aromatic molecular structure making it an inert and non-biodegradable substance [1]. When this non-biodegradable substance being release to the environment, it tends to accumulate in water streams for long period of time. This builds up prompt the production of toxic by-product which is extremely harmful and alarming to both human and environment. Moreover, MB dye can also cause alarming health issues to human being, such as high blood pressure, nausea, shock, mental confusion, and vomiting [2]. With that information, the removal synthetic dyes from wastewater are an urgent matter that need to be address.

Conventional techniques that are commonly used to remove synthetic methylene blue dye from wastewater were chemical degradation, membrane separation, coagulation and flocculation, oxidation, precipitation, and adsorption. Among these techniques, adsorption process is one of the most implemented techniques for the removal of synthetic dyes compared to others conventional methods that have limitations such as produce secondary effluents, uses high temperature and pressure, complex process with advanced instrumentation, and in need of skilful labour. On contrary, the adsorption techniques are considered economically feasible, simple, and easy to handle, have vast availability of adsorbent and better removal efficiency. Most importantly, activated carbon was effective in treating various pollutants such as dyes [3-4], heavy metals [5-6], phenol [7] and others. Despite that, the commercially used activated carbon precursor such as coal is quite expensive and too costly for wastewater treatment process. Therefore, the search for alternative AC precursor from renewable sources is a call for. Tremendous research initiatives have been studied to synthesize AC from renewable sources especially biomass waste such as teak wood [8], almond shell [9], meranti wood [10], acacia mangium wood [7], *hevea brasillies* root [11], *moringa oleifeira* [12], lemongrass leaves [13], coconut shell [5] and others.

In choosing the precursor material for activated carbon preparation, several factors need to be considered such as the availability of raw material, non-hazardous nature, and production cost. These days, biomass has been extensively used as a precursor for AC production because of its environmentally friendly nature. Therefore, in this work, an abundantly available agricultural waste rice husk (RH) was employed to fabricate an activated carbon using microwave radiation activation technique for the MB removal from aqueous solution. Not only abundantly available at low cost, two major components in rice husk such as carbon and silica also an excellent property for it to be considered as an adsorbent precursor because these properties will contribute to the production of highly porous and excellent specific surface area adsorbent. Meanwhile, the microwave activation process was used because it is a quick, convenient and feasible activation method that can successfully convert biomass waste into porous AC with great performance [8]. The preparation conditions of RHAC were optimized utilizing response surface methodology (RSM). Characterization was done on the RHAC to evaluate its properties. Eventually, the MB removal, isotherms, and kinetics analysis was done through batch adsorption studies where adsorbate initial concentration, contact time, and solution temperature were varied.

Materials and Methods

Materials

The agricultural waste rice husk (RH) precursor was procured from a local rice factory situated in Perak, Malaysia. The Methylene blue (MB) adsorbate was purchased from Sigma-Aldrich (M) Sdn. Bhd, Malaysia. Meanwhile, the gases for both carbonization and activation process; CO_2 and N_2, were provided by MOX Gases Berhad, Malaysia.

Preparation of Rice Husk Based Activated Carbon (RHAC)

The rice husk precursor was washed and dried in the sun as a pre-treatment to remove any visible impurities. Then, it was further dried at temperature of 110 °C in an oven for 48 h to remove the remaining moisture. Dried rice husk was then subjected to carbonization process using a vertical furnace. Throughout this process, N_2 gas was passed along the vertical furnace. Resulted char from carbonization process was then undergo microwave irradiation activation process using modified microwave. The activation process was carried out at radiation power of 440 Watt for 4.28 minutes. Throughout the microwave activation process, CO_2 gas at flow rate of 150 cm^3/min was continuously flowed across the microwave. The resulted product at the end of the process is called RHAC.

The optimized operating conditions was obtained from Design Expert software (STAT.EASE Inc. Minneapolis, USA) where a standard response surface methodology (RSM) design called central composite design (CCD) was used to study the parameter in the preparation of activated carbon and the procedure was similar to the previous work [6]. This design develops a polynomial regression model developed to analyse the correlations of the AC preparation variables such as radiation power (X_1) and radiation time (X_2) with two responses, methylene blue removal (Y_1) and RHAC yield (Y_2). Equation 1 represents the standard form of the quadratic model generated by RSM,

$$Y = b_0 + \sum_{i=1}^{n} b_i x_i + \left(\sum_{i=1}^{n} b_{ii} x_i\right) + \sum_{i=1}^{n-1} \sum_{j=i+1}^{n} b_{ij} x_i x_j \qquad (1)$$

where:

Y = Predicted response,
b_0 = Constant coefficient,
b_i = Linear coefficient,
b_{ij} = Quadratic coefficient,
x_i, x_j = Coded value of the AC.

The models were evaluated based on the correlation coefficient, R^2.

Characterizations

The functional groups of rice husk precursor and RHAC synthesized was evaluated using FTIR spectrophotometer (Model: IR Prestige 21 Shidmazu, Japan). The surface chemistry was assessed using simultaneous thermal analyzer (Perkin Elmer STA 6000, USA) and elemental analyzer (EA) (Model Perkin Elmer Series II 400, USA). Meanwhile, the surface features of the RHAC were evaluated by Micromeritics ASAP 2020 volumetric adsorption analyzer and the Brunauer-Emmet-Teller (BET) analysis. Lastly, the scanning electron microscope (LEO SUPRA 55VP, Germany) analysis was performed to evaluate the morphological surface of the raw rice husk and RHAC adsorbent.

Batch Equilibrium, Isotherms and Kinetics Studies

Batch equilibrium study at different conditions were opted for the MB adsorption. Initial dye concentration (25 mg/L to 300 mg/L), contact time (0 to 24 h) and different solution temperature (30 °C, 45 °C and 60 °C) were studied where the MB adsorption uptakes and percentage removal were evaluated. During batch experiment, 0.20 g RHAC was added into 200 mL MB dye solution in an Erlenmeyer flask. Then, it was placed into a water bath shaker and agitated at 150 rpm for 24 h to allow the adsorption process to occur. To determine the adsorption uptakes and removal efficiency of the adsorbates, Equations 2 and 3 were used:

$$q_e = \frac{(C_o - C_e)V}{M} \tag{2}$$

$$Removal\ (\%) = \frac{(C_o - C_e)}{C_o} \times 100\% \tag{3}$$

The q_e in Equation 1 represent the number of adsorbates at equilibrium (mg/g). C_o and C_e represent the MB initial concentration and MB concentration at equilibrium (mg/L). V (mL) is the solution volume and M (g) is the mass of the activated carbon used. For isotherms study, the data obtained from batch experiments was fitted into 3 isotherms model: Langmuir, Freundlich and Temkin. The linearized isotherms equation used were expressed in Equations 4, 5 and 6 for Langmuir, Freundlich and Temkin model, respectively. The best-fitted isotherms were determined through the value of correlation coefficient, R^2 which closest to the unity.

$$\frac{C_e}{q_e} = \frac{1}{q_m} C_e + \frac{1}{K_L q_m} \tag{4}$$

$$\ln q_e = \frac{1}{n_F} \ln C_e + ln\ K_F \tag{5}$$

$$q_e = B \ln C_e + B \ln A_t \tag{6}$$

where:

C_e = Equilibrium concentration of adsorbate (mg/L)
q_e = Amount of adsorbate adsorbed at equilibrium (mg/g)
q_m = Monolayer adsorption capacity of the adsorbent (mg/g)
K_L = Langmuir adsorption constant (L/mg)
$1/n_F$ = Adsorption intensity
K_F = Freundlich isotherm constant (mg/g(L/mg)$^{1/n}$)
R = Universal gas constant (8.314 J/mol K)
T = Absolute temperature (K)
A_t = Equilibrium binding constant (L/mg)
B = RT/b = constant related to the heat of adsorption (L/mg)

Meanwhile, pseudo-first order and pseudo-second order models (Equations 7 and 8, respectively) were implemented for the kinetic analysis. This analysis evaluates the performance of a given adsorbent to gain insight into the underlying adsorption mechanism. The value of correlation coefficient, R^2 for both isotherms and kinetic analysis was evaluated to describe the methylene blue dye adsorption system on the RHAC.

$$\ln(q_e - q_t) = \ln q_e - K_1 t \tag{7}$$

$$\frac{t}{q_t} = \frac{1}{k_2 {q_e}^2} + \frac{1}{q_e} t \tag{8}$$

where:

q_t = Amount of adsorbate adsorbed at time t (mg/g)
q_e = Amount of adsorbate adsorbed at equilibrium (mg/g)
K_1 = Pseudo-first order rate constant of adsorption (1/h)
K_2 = Pseudo-second order rate constant of adsorption (g/mg.h)

Sample Analysis

For adsorbates concentration analysis, a calibration curve was obtained to ensure the homogeneity of the absorbance when various concentrations of adsorbates were being measured. A set of varies MB's concentration was prepared, and their absorbance was measured using UV-Vis spectrophotometer (Model Shimadzu UV-1800, Japan) at wavelength of 663 nm to construct a calibration curve where the Beer-lambert relationship between absorbance and concentration was plotted in graph of absorbance versus concentration of the dye solutions. During batch adsorption study, the sample of methylene blue adsorbates was taken from the batch adsorption solution at a set time intervals using 3 mL disposable syringe. The sample taken was then measured using UV-Vis spectrophotometer at wavelength of 663 nm where the absorbance obtained was compared with the calibration curve plotted earlier to determine the concentration of the methylene blue adsorbates.

Results and Discussion

Optimization Study of AC Yield and MB Dye Removal

Polynomial regression model developed using a standard response surface methodology (RSM) design called a central composite design (CCD) was utilized to analyse the correlations of the AC preparation variables, radiation power (X_1) and radiation time (X_2) and two responses, MB removal (Y_1) and RHAC yield (Y_2). It was found that the range of MB removal was within 70.96 % to 94.12 %, while for RHAC yield it was ranging from 19 % to 44.33 %. Based on the software suggestions, a quadratic model was selected to represent MB removal, whereas a linear model was utilized for RHAC yield to correlates the data to the responses. According to the statistical analysis, the final empirical model for the MB removal and RHAC yield responses obtained by RSM are shown in Equations 9 and 10.

MB dye removal, Y_1:

$$Y_1 = 89.99 + 7.84X_1 + 3.87X_2 - 1.40X_1X_2 - 3.38{X_1}^2 - 3.69{X_2}^2 \tag{9}$$

RHAC's yield, Y_2:

$$Y_2 = 30.36 - 5.99X_1 - 2.55X_2 \tag{10}$$

Validation and suitability of the created models above were assessed by looking at the R^2 value and its standard deviation value. Most suited and valid model will exhibit a high value of R^2 that approaching unity as it is competent to anticipate the responses better based on the parameters. Indeed, the models develop for both Equations 9 and 10 gave high R^2 value of 0.9546 and 0.9052, respectively. The proximity of these R^2 values to unity indicated that the predicted value for MB removal and RHAC yield, was near to the experimental values. In addition, the R^2 values also reflected the contributions of the variable's studies on the total variations in MB dye removal and RHAC's yield, which was 95.46 % and 90.52 % respectively. On top of that, low standard deviations of 2.29 and 3.10 was calculated for both model in Equations 9 and 10, respectively, indicated a low deviation of predicted data from the actual experimental data. Therefore, further justify the compatibility of the experimental values and the model predicted values. For that reason, it could be presumed that the developed models using CCD had successfully provided an adequate and satisfying prediction for both MB removal and RHAC yield responses.

Table 1 provides the optimum RHAC preparation conditions with the best desirability that leads to highest response of MB removal and RHAC's yield generated by Design Expert software. The most ideal conditions for RHAC preparation were found to be at radiation power of 440 W and radiation time of 4.28 minutes, with MB removal of 83.93 % and RHAC yield of 32.55 %. Experimental runs were conducted to validate the accuracy of the optimized conditions generated by the software, which resulted in MB removal of 83.05 % and RHAC's yield of 31.98 %. Based on the predicted and actual experimental results, a low error percentage of 1.05 % and 1.75 % was obtained for both MB removal and RHAC's yield responses, respectively.

Table 1: Model validation for RHAC preparation

AC	**Radiation power, X_1 (W)**	**Radiation time, X_2 (min)**	**MB removal (%)**			**RHAC yield (%)**		
			Predicted	**Actual**	**Error (%)**	**Predicted**	**Actual**	**Error (%)**
RHAC	440	4.28	83.93	83.05	1.05	32.55	31.98	1.75

Analysis of Variance (ANOVA)

To validate the predictive quality of the suggested model, analysis of variance (ANOVA) was implemented. The ANOVA results for the quadratic model of MB removal and linear model of RHAC yield was provided in Table 2 and Table 3, respectively. The significance of the model was evaluated by high F-value and Prob > F value that is less than 0.05 [14]. For this case, the F-value for both MB removal and AC yield responses were considered high at 29.45 and 17.65, respectively. While Prob > F value were at 0.0001 and 0.0005, respectively, therefore proved that the model was not random and significant to the responses. According to Table 1, the terms that were found to be significant in the MB removal model were unifactor effect of X_1, X_2, and quadratic effect X_1^2, X_2^2. While double factor effect of X_1X_2 was not significant since F-values was lower and Prob > F value are greater than 0.05 compared to other terms. On the other hand, for RHAC's yield, both unifactor effect of X_1 and X_2 process parameters was significant to the responses studied.

These make sense as radiation power (X_1) was high or radiation time (X_2) was prolonged, more pores and active sites were able to form and available for MB dye particle to be adsorbed. However, when the radiation power and time reached a certain maximum value, the microwave heating process would burn off the carbon pores and destroyed the structure, thus affecting both RHAC's yield and MB adsorption.

Table 2: ANOVA for MB dye removal by RHAC

Source	Sum of squares	Degree of freedom (DF)	Mean square	F-Value	Prob > F
Model	774.44	5	154.89	29.45	0.0001
X_1	492.09	1	492.09	93.55	<0.0001
X_2	120.11	1	120.11	22.83	0.0020
X_1X_2	7.87	1	7.87	1.50	0.2609
X_1^2	79.64	1	79.64	15.14	0.0060
X_2^2	94.77	1	94.77	18.02	0.0038

Table 3: ANOVA for RHAC's yield

Source	Sum of squares	Degree of freedom (DF)	Mean square	F-Value	Prob > F
Model	339.18	2	169.59	17.65	0.0005
X_1	287.32	1	287.32	29.90	0.0003
X_2	51.09	1	51.85	5.40	0.0426

Three-dimensional surface response and contour plots were constructed to explore the relationships between selected variables and responses of the models. Figure 1(a) depicted the 3D surface responses of MB removal under the effect of radiation power and radiation time. According to 3D parabolic shape plots of MB dye removal in Figure 1(a), the dye removal increases with the increase of radiation power up to the optimum value. Then, further increased of the radiation power beyond the optimum limit showed a slight drop in MB removal response. Vice versa, poor response recorded was at the lowest radiation power and radiation time. This trend is cause by the successful pore formation at high microwave power and activation time. High temperatures and prolonged activation times gave sufficient time for the volatile matters to burn out and created a highly porous carbon with numerous active sites for MB removal. An equivalent trend has been reported in previous work by Aziz and Hassan [15], using Parkia speciosa pod based activated carbon, where it was found that the increases of microwave power to a certain optimum value does increased the removal % and decreases when the power goes beyond the optimum limit. Meanwhile, for RHAC yield, Figure 1(b) shows that effect of both radiation power and radiation time were significant on the response where radiation power imposed pronounced effect than the radiation time. The highest RHAC yield was recorded when it was prepared at lowest radiation power and radiation time as can be interpreted from Figure 1(b). The results are plausible because at low operating conditions, less microwave energy being impinged on the AC as well as less devolatilization rate occur. Therefore, hindered the pore formation process and the released of volatile matter which restored the RHAC yield.

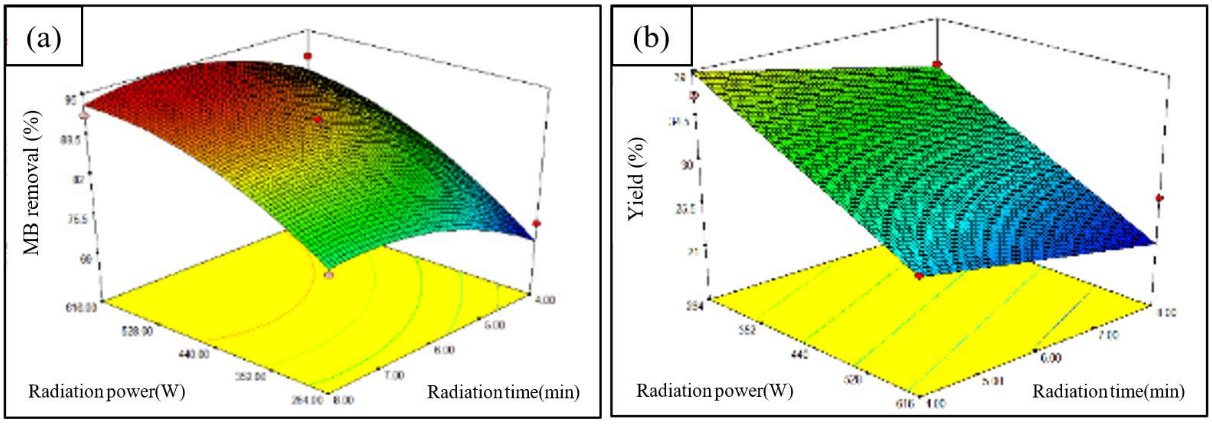

Figure 1: 3D response plot - Influence of radiation power and radiation time for (a) MB dye removal and (b) RHAC yield

Characterizations

FTIR was used to characterized and evaluate the surface functionality the synthesized RHAC as well as the raw rice husk precursor. Figure 2 displayed the FTIR spectra of both rice husk precursor and RHAC adsorbent synthesized.

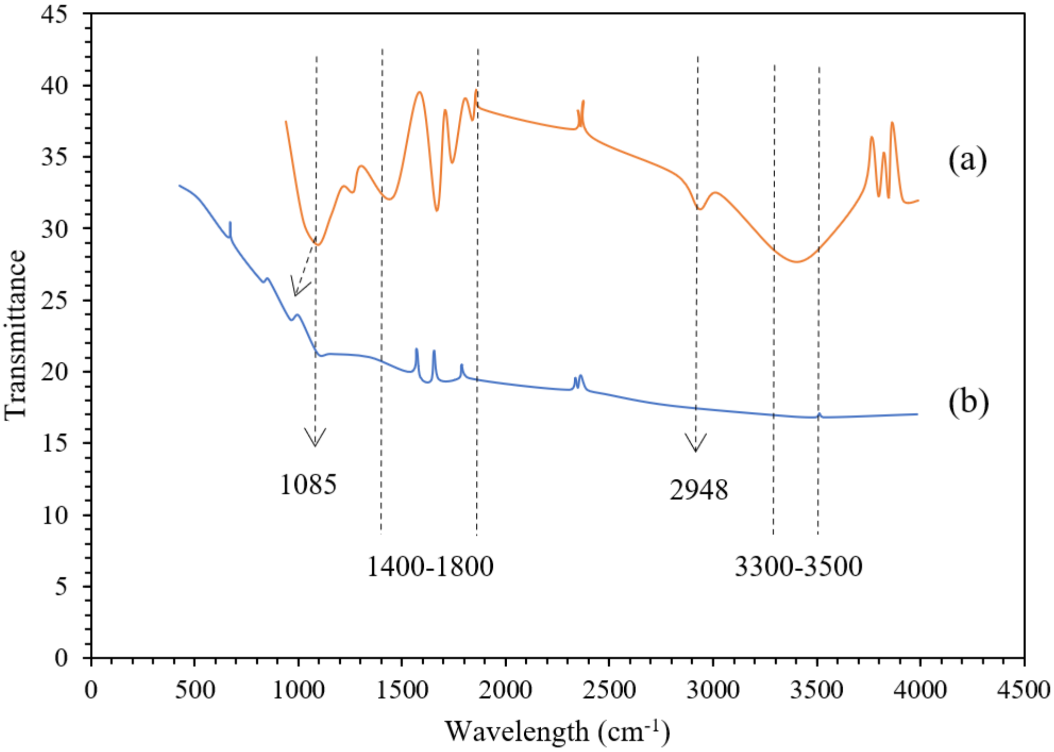

Figure 2: FTIR spectra of (a) rice husk and (b) RHAC

From the FTIR spectra, the wide broad band appeared around 3300 cm^{-1} to 3500 cm^{-1} on rice husk spectra were assigned to stretching vibration of hydroxyl groups, O-H. Meanwhile, the weak band observed at 2948 cm^{-1} attributed to the symmetric and asymmetric vibration of C–H stretching in alkane groups. However, both O-H and C-H stretching was not available on RHAC spectra. This may be due to the moisture lost and volatilization of organic component during carbonization and activation process. Besides that, a numerous band represented the carbonyl C=O (aldehydes, ketones, lactones), carboxyl -COOH, and alkanes stretching vibrations were also observed between 1400 cm^{-1} to 1800 cm^{-1} on both rice husk and RHAC spectra. These bands were expecting to contribute to the MB adsorption. In addition to that, a distinct peak on rice husk spectra was also seen at 1085 cm^{-1} which may be corresponded to the stretching vibrations of carbonyl group, C=O. This peak was slightly shifted to 958 cm^{-1} due to the modification of surface chemistry under microwave heating during activation process. In short, all the oxygen-containing functional groups such as C=O and -COOH discovered in the FTIR analysis are significant as it play an important role of providing an active sites in adsorption process [10]. Several interactions were possible with the present of these functional groups on AC's active sites include an electrostatic interaction between deprotonated carboxyl group on AC surface with the positively charged MB cations because the oxygen atoms have large affinity towards positively charged molecules such as MB ions [16]. Besides that, hydrogen bonding may also occur between carboxyl and carbonyl group on the activated carbon surface and the MB's H-bond acceptor. Nonetheless, π-π stacking interaction is also favourable between aromatic groups in AC and MB molecules due the rich aromatic rings structure of the cations.

Results for proximate and elemental analysis were given in Table 4. It was found that the fixed carbon content in rice husk was relatively high for biomass at 23.69 %, therefore making it suitable to be use as activated carbon precursor. Moreover, the fixed carbon percentage of RHAC tremendously increased to 70.34 %, while both moisture and volatile matter were reduced to 5.74 % and 14.19 %, respectively. It was obvious that heat treatment in the preparation process affecting the organic compound present in the rice husk, which leads to the breakdown of lignocellulosic materials and volatilization of the volatile compound [17]. As a result, an adsorbent with high carbon percentage was produced. Aside from that, the proximate analysis also showed a low percentage of ash at 1.91 %, which was desirable because it indicates the heat treatment in both carbonization and microwave activation process was in the right range and no combustion occurs. Meanwhile, elemental results demonstrated that RHAC consists of 75.60 % carbon (C), 3.02 % hydrogen (H), 0.10 % sulphur (S) and 21.28 % combination of nitrogen and oxygen (N+O). The variety type of functional groups present was a good indication as it is important to improve the MB adsorption process as discussed before in the FTIR results.

Table 4: Proximate and elemental analysis of rice husk precursor and RHAC

Sample	**Proximate analysis (%)**				**Elemental analysis (%)**			
	Moisture	**Volatile**	**Fixed Carbon**	**Ash**	**C**	**H**	**S**	**(N+O)[a]**
RH	10.88	57.82	23.69	2.35	28.11	8.51	0.25	63.13
RHAC	5.74	14.19	70.34	1.91	75.60	3.02	0.10	21.28

[a] Estimated by difference

Physical properties of the RHAC synthesized was evaluated in BET analysis using N_2 adsorption/desorption technique. The results are presented in Table 5. The BET surface area was noticed to increase from 1.45 m^2/g to 668.30 m^2/g for rice husk and RHAC, respectively. Meanwhile, the average pore diameter is about 4.42 nm and it was found to represent a mesopores structure with mesopore surface area of 435.17 m^2/g. Mesopores structure and high surface area suggested a better adsorption capacity toward targeted adsorbates. Pores formation phenomena occurs during activation process. The microwave energy adsorbed by the electron in the raw rice husk during activation process rotated at high speed and dissipated the energy to the entire sample leads to the removal of moisture and volatile matter within the precursor [6]. Thus, this signified the successful formation of mesopores structure.

Table 5: Surface and pore characteristics of rice husk precursor and RHAC

Sample	BET surface area (m^2/g)	Mesopore surface area (m^2/g)	Total pore volume (cm^3/g)	Average pore diameter (nm)
RH	1.45	-	-	-
RHAC	668.30	435.17	0.35	4.42

(-) not available

SEM analysis was utilized to evaluate the surface morphology of the RHAC produced. Figure 3 revealed the SEM micrograph for rice husk and RHAC synthesized. From the images, it can be clearly seen that the surface of rice husk was uneven, relatively rough and no pores were visible. In contrast, RHAC demonstrated a significant structure change with a visible porous structure. The entire RHAC was filled with cavities of pores distributed evenly throughout the surface. The formation of surface pores could be explained through kinetic point of view where the volatilization of moisture and volatile matter were emphasized as discussed before in the BET analysis. Importantly, the developed pores promote the penetration of organic compounds like MB dye within the RHAC matrix. Thus, the SEM images confirmed the ability of RHAC prepared via microwave activation to be used for MB adsorption process.

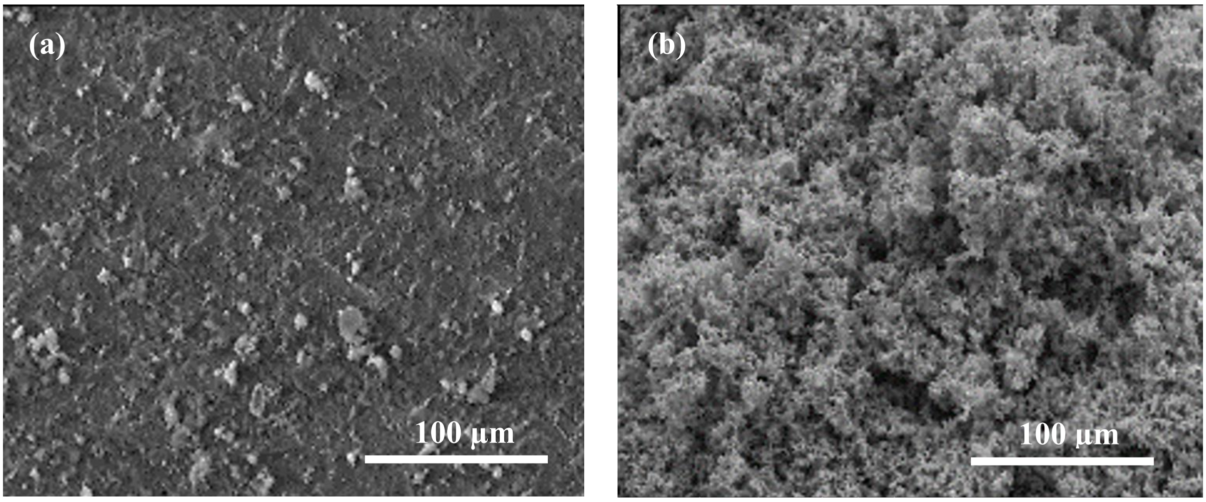

Figure 3: SEM micrographs of (a) rice husk and (b) RHAC

Batch Equilibrium Studies: Effect of Initial MB Concentration, Contact Time and Solution Temperature on Adsorption Process.

Batch equilibrium studies were done to assess the effect of MB initial concentration, contact time, and solution temperature on the adsorption uptakes and removal efficiency. All results were plotted in Figure 4. From the outcome, Figure 4(a) demonstrated an increase in adsorption uptake, q_t and removal percentage with the increase of contact time until the equilibrium was reached. It was also important to point out that the adsorption uptakes and removal of MB dye was faster at first 5 h and it seemed to slow down as the time prolonged and reached equilibrium. The MB uptakes and removal was faster at earlier stage was because of the availability of vacant fresh active sites at the beginning. Thus, leads to rapid adsorption of adsorbates onto the available sites at first 5 hour of adsorption process. However, the uptakes become slower after 5 hours since the active sites become occupied and the repulsion between the MB adsorbates on the adsorbent and the bulk phase causes the remaining surface sites difficult to be occupied. Towards the end, the adsorption process continued at slower rate until it reached equilibrium.

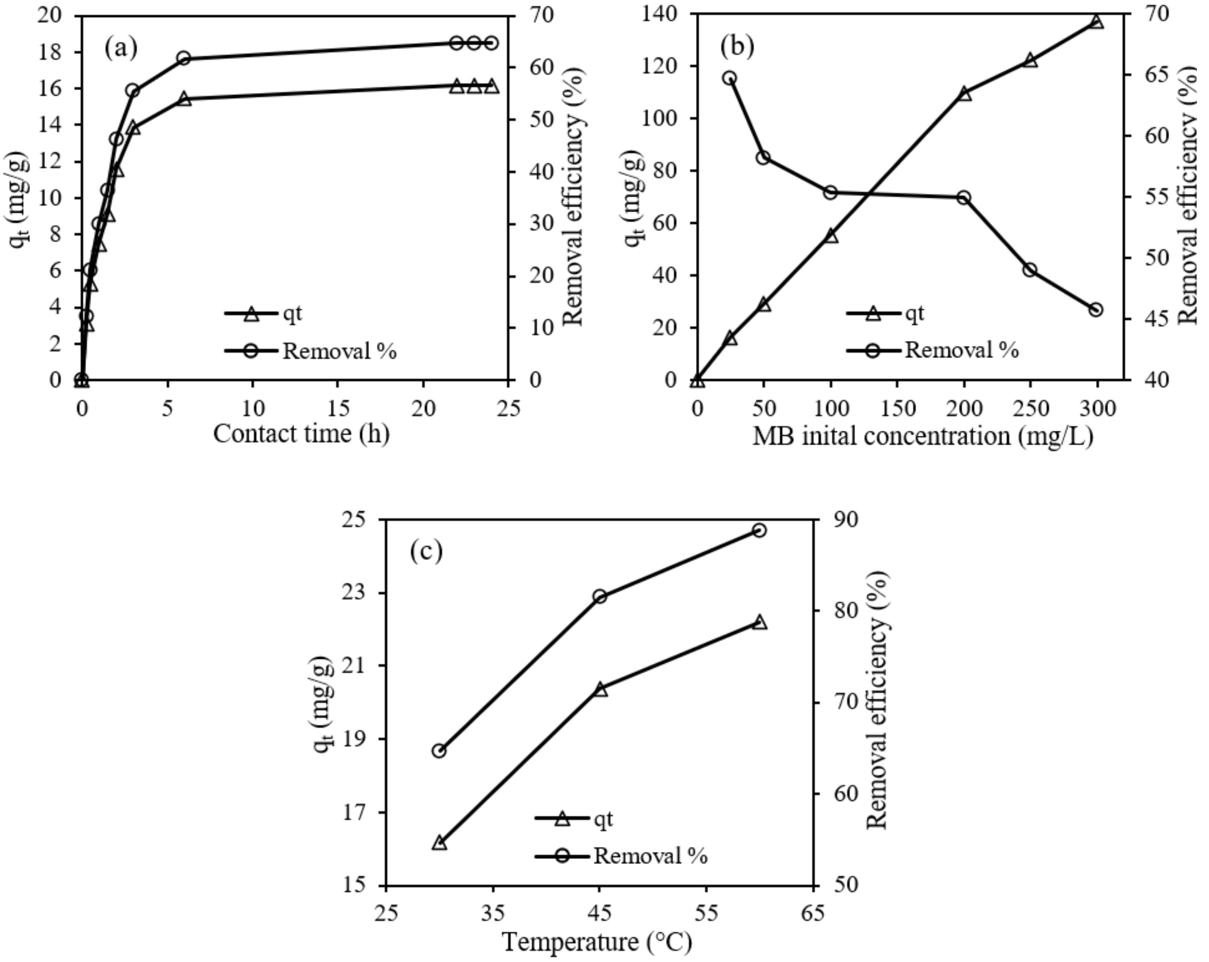

Figure 4: The influence of (a) contact time (fixed: 25 mg/L initial concentration, 30 °C), (b) dye initial concentration (fixed: 24 h contact time, 30 °C) and (c) solution temperature (fixed: 25 mg/L initial MB concentration, 24 h contact time) on the adsorption uptake and MB removal efficiency

The impact of MB dye initial concentration on adsorption uptakes and removal percentage can be observed in Figure 4(b). As the initial dye concentration increased from 25 mg/L to 300 mg/L, that the adsorption uptakes were found to increase as well. However, the removal efficiency was discovered to reduced when initial MB dye concentration was increased. The increases in adsorption uptakes can be explained by the greater concentration gradient that acts as a promoter that drive MB dye adsorption onto RHAC active sites. At high initial concentration, the number of adsorbates molecules were higher therefore leads to a greater mass transfer between the adsorbate molecules in the bulk solution onto the solid adsorbent phase. Thus, increases the adsorption rate as more adsorbates available to compete for vacant active sites which eventually increases the MB dye adsorption uptakes. However, since the ratio of MB molecules to available adsorption sites was high at higher initial concentration, bigger percentage of MB molecules was unable to be adsorbed due to the limited vacant active sites available, thus explaining the drop of MB removal percentage at higher initial concentration [8].

On the other hand, Figure 4(c) showed an increased in both adsorption uptakes and removal percentage as the solution temperature rises. This means that the adsorption reaction was endothermic which enhanced at higher temperature. The improvement in adsorption uptakes and removal efficiency at higher solution temperature may be attributed to energy gains by the adsorbate molecules as heat supplied was increased. More energy acquired enhanced the interaction between the adsorbate's molecules with adsorbent active sites during adsorption process, therefore promotes the bond formation such as hydrogen bonding, electrostatic interaction and π-π stacking interaction with the functional groups on the AC's surface discovered in the FTIR results.

Adsorption Isotherms

Adsorption isotherm study was done to examine the adsorbates adsorption mechanism that occurred on the RHAC adsorbent surface. In this study, the linearized form of three well-known isotherm models, Langmuir, Freundlich and Temkin (Equation (4), (5) and (6), respectively) were applied to fit the experimental data. These isotherm models demonstrate the phenomena that occurred at the adsorbent surface during adsorption process. For instance, Langmuir isotherm represents a homogeneous and monolayer adsorption of adsorbate on the outer surface of the adsorbent, while Freundlich isotherm model assumes the multilayer coverage of adsorbates on rough and heterogonous surface. Temkin model consider the interaction between adsorbent and adsorbates where the extremely large and low concentration values were ignores. Temkin's assume that the adsorption heat would decrease linearly with surface coverage. Figures 5(a), (b) and (c) plotted the linearized Langmuir, Freundlich and Temkin isotherm models at different solution temperature, respectively.

Meanwhile, the isotherm parameters for MB adsorption were tabulated in Table 6. From Table 6, the result shows that Freundlich isotherm model fit the experimental data the best with highest coefficient of determination, R^2 values above 0.98 at all temperatures, which was better than Langmuir and Temkin isotherm model. This indicates the occurrence of multilayer adsorption process of adsorbates MB molecules onto the heterogeneous surface of RHAC adsorbent [18]. Furthermore, the n_F value that closer to 1 in Freundlich model are favourable for MB-RHAC adsorption system as it signified a good efficiency for MB adsorption by the adsorbent [19].

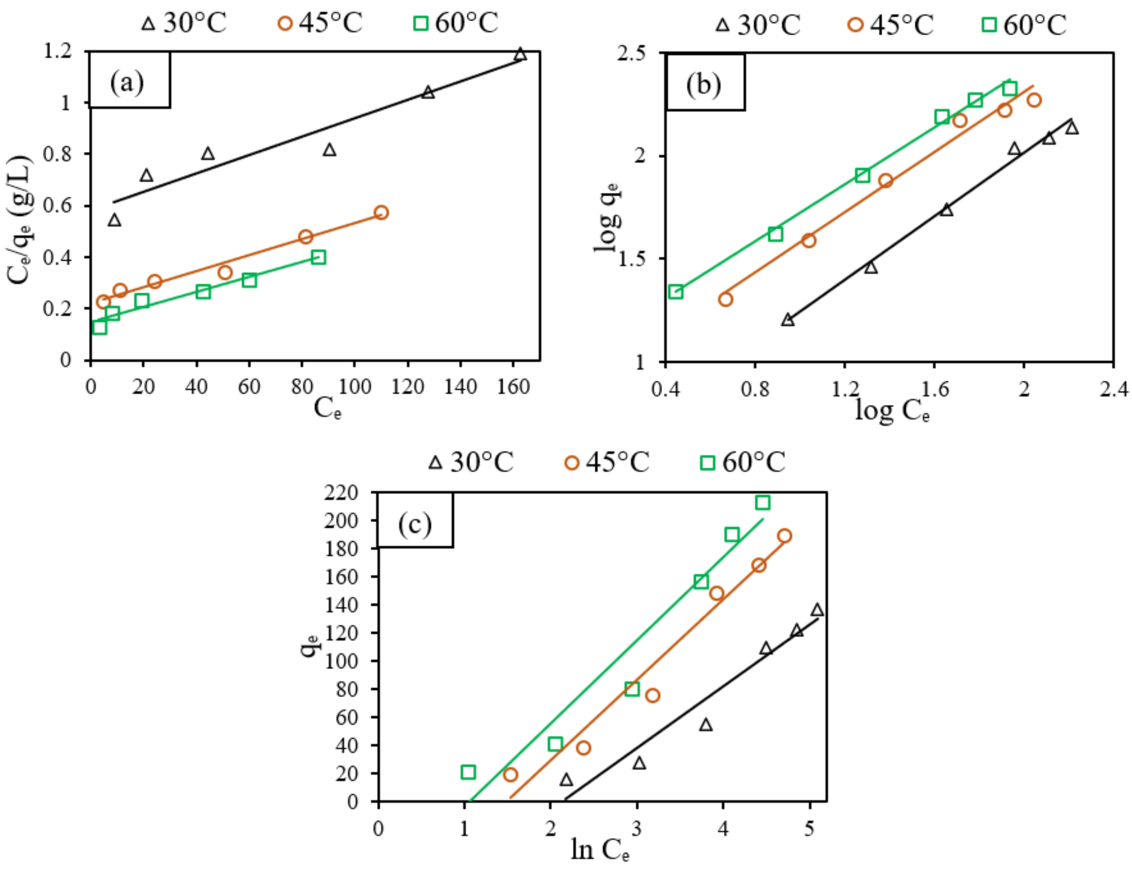

Figure 5: Linearized plots of (a) Langmuir, (b) Freundlich and (c) Temkin isotherms for MB-RHAC adsorption at 30 °C, 45 °C and 60 °C

Table 6: Isotherm parameters for MB adsorption

Isotherms	Temperature (°C)	Constants		R^2
		q_m	K_L	
Langmuir	30	277.78	0.01	0.92
	45	322.58	0.01	0.97
	60	344.83	0.02	0.96
		k_F	n_F	
Freundlich	30	3.00	1.30	0.99
	45	7.05	1.37	0.98
	60	10.78	1.45	0.99
		A	B	
Temkin	30	0.12	44.14	0.94
	45	0.23	57.15	0.96
	60	0.35	59.05	0.94

Kinetic Study

To understand the mechanism, MB diffusion process and its controlling step during adsorption process, kinetic assessment was made using two different kinetic models; PFO and PSO (Equation (7) and (8)). PFO assumed that rate of the adsorption process is directly proportional to the fluctuation between q_e and q_t which indicates a physical adsorption mechanism, while PSO kinetics indicates a chemisorption mechanism. Figure 6 presents the kinetic plot of PFO and PSO for MB-RHAC adsorption at 30 °C.

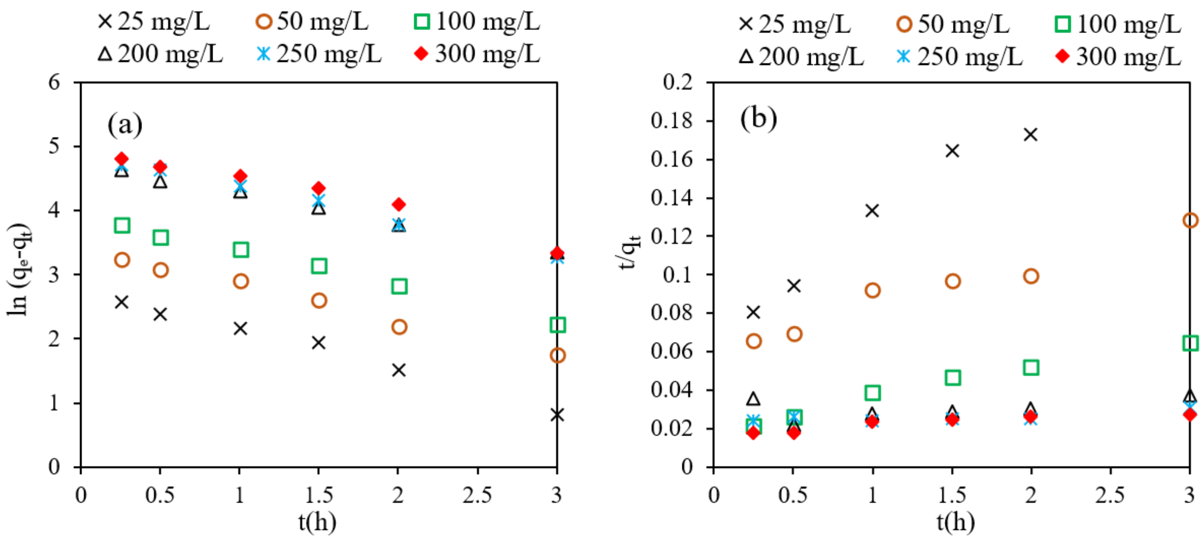

Figure 6: Kinetic plots of (a) PFO and (b) PSO for MB adsorption at 30 °C

On the other hand, Table 7 tabulates the kinetic model parameters for the MB-RHAC adsorption system. From the results, it was obvious that PFO model fitted the MB adsorption kinetic the best with higher R^2 values up to 0.99 compared to PSO. Moreover, the $q_{e,calc}$ from PFO model also in agreement with the $q_{e,exp}$ from the experimental data, therefore further confirmed that the kinetic data was well presented by PFO model. The important findings from this kinetic study were that PFO suggested a physical adsorption mechanism for the MB-RHAC adsorption system [20]. The physical adsorption is mainly carried out through nonbonding (steric) interactions, Van der Waals forces, or hydrogen bond interactions. When weak forces such as Van der Waals forces hold the adsorbates solute to the solid adsorbent surface, a rapid equilibrium can be achieved, and it is easily reversible due to the small energy requirement.

Table 7: Kinetic model parameters for MB-RHAC system at 30 °C

Initial MB concentration, C_o(mg/L)	**q_e, exp. (mg/g)**	**Pseudo-first order**			**Pseudo-second order**		
		q_e, calc (mg/g)	**k_1**	**R^2**	**q_e, calc (mg/g)**	**k_2**	**R^2**
25	16.18	15.80	0.62	0.99	20.41	0.03	0.97
50	29.12	29.59	0.55	0.99	45.66	0.01	0.95
100	55.35	50.34	0.55	0.99	63.29	0.01	0.98
200	109.85	114.62	0.47	0.99	416.67	0.00	0.21
250	122.35	133.78	0.54	0.99	454.55	0.00	0.68
300	137.15	150.20	0.51	0.96	256.41	0.00	0.84

Conclusions

This research demonstrated the great potential of rice husk as an adsorbent precursor in fabrication of high-performance AC for MB dye adsorption. Experimental design, RSM results revealed that the optimum RHAC preparations conditions for microwave radiation was at 400 W while activation time was at 4.28 minutes. Both resulted in 83.93 % MB removal and 32.55 % RHAC yield. Microwave radiation activation technique also had successfully synthesized a high carbon content RHAC with excellent physical properties such as a mesoporous type of pore structure with average pore diameter of 4.42 nm, excellent BET surface area of 668.30 m^2/g, and pore volume of 0.35 cm^3/g. Furthermore, the RHAC was also packed with variety types of functional groups that were beneficial for MB dye adsorption. In batch equilibrium studies, high adsorption uptakes and removal efficiency was obtained at longer contact time and higher solution temperature. In contrary, high MB initial concentration decreases the removal efficiency of MB dye adsorption. Lastly, isotherms and kinetic evaluation determined that the adsorptions of MB on the RHAC surface were best suited the Freundlich isotherm model and most fittingly represented by the pseudo-first order kinetic model.

Acknowledgements

An appreciation is given to Ministry of Higher Education Malaysia that supported this research work under Fundamental Research Grant Scheme (FRGS/1/2021/TK0/USM/01/3). Besides that, the authors also would like to recognize Universiti Sains Malaysia for the technical and facilities support.

Author Contributions

All authors contributed toward data analysis, drafting and critically revising the paper and agree to be accountable for all aspects of the work.

Disclosure of Conflict of Interest

The authors have no disclosures to declare

Compliance with Ethical Standards

The work is compliant with ethical standards

References

[1] Kenawy, E. -R., Tenhu, H., Khattab, S. A., Eldeeb, A. A. & Azaam, M. M. (2022). Highly efficient adsorbent material for removal of methylene blue dye based on functionalized polyacrylonitrile. *European Polymer Journal*. 169, 111138.

[2] El Bouazzaoui, Y., Habsaoui, A. & Touhami, M. E. (2022). Hydrogel synthesis using extracted cellulose from Opuntia Ficus indica seeds and its application in methylene blue dye removal. *Chemical Data Collections*. 41, 100918.

[3] Khasri, A. & Ahmad, M. A. (2018). Adsorption of basic and reactive dyes from aqueous solution onto Intsia bijuga sawdust-based activated carbon: batch and column study. *Environmental Science and Pollution Research*. 25(31), 31508-31519.

[4] Yusop, M. F. M., Ahmad, M. A., Rosli, N. A., Gonawan, F. N. & Abdullah, S. J. (2021). Scavenging malachite green dye from aqueous solution using durian peel based activated carbon. *Malaysian Journal of Fundamental and Applied Sciences*. 17(1), 95-103.

[5] Yusop, M. F. M., Mohd Johan Jaya, E., Mohd Din, A. T., Bello, O. S. & Ahmad, M. A. (2022). Single-Stage Optimized Microwave-Induced Activated Carbon from Coconut Shell for Cadmium Adsorption. *Chemical Engineering & Technology*. 45(11), 1943-1951.

[6] Yusop, M. F. M., Jaya, E. M. J. & Ahmad, M. A. (2022). Single-stage microwave assisted coconut shell based activated carbon for removal of Zn(II) ions from aqueous solution – Optimization and batch studies. *Arabian Journal of Chemistry*. 15(8), 104011.

[7] Alam, M. G., Danish, M., Alanazi, A. M., Ahmad, T. & Khalil, H. P. S. A. (2023). Response surface methodology approach of phenol removal study using high-quality activated carbon derived from H_3PO_4 activation of Acacia mangium wood. *Diamond and Related Materials*. 132, 109632.

[8] Firdaus Mohamad Yusop, M., Aziz, A. & Azmier Ahmad, M. (2022). Conversion of teak wood waste into microwave-irradiated activated carbon for cationic methylene blue dye removal: Optimization and batch studies. *Arabian Journal of Chemistry*. 15(9), 104081.

[9] Saka, C., Teğin, İ. & Kahvecioğlu, K. (2023). Sulphur-doped carbon particles from almond shells as cheap adsorbent for efficient Cd(II) adsorption. *Diamond and Related Materials*. 131, 109542.

[10] Mohamad Yusop, M. F., Tamar Jaya, M. A., Idris, I., Abdullah, A. Z. & Ahmad, M. A. (2023). Optimization and Mass Transfer Simulation of Remazol Brilliant Blue R Dye Adsorption onto Meranti Wood Based Activated Carbon. *Arabian Journal of Chemistry*. 16(5), 104683.

[11] Ahmad, A. A., Ahmad, M. A., Yahaya, N. K. E. M. & Karim, J. (2021). Adsorption of malachite green by activated carbon derived from gasified Hevea brasiliensis root. *Arabian Journal of Chemistry*. 14(4), 103104.

[12] Khalfaoui, A., Bouchareb, E. M., Derbal, K., Boukhaloua, S., Chahbouni, B. & Bouchareb, R. (2022). Uptake of Methyl Red dye from aqueous solution using activated carbons prepared from *Moringa Oleifera* shells. *Cleaner Chemical Engineering*. 4, 100069.

[13] Ahmad, M. A., Ahmed, N. B., Adegoke, K. A. & Bello, O. S. (2021). Adsorptive potentials of lemongrass leaf for methylene blue dye removal. *Chemical Data Collections*. 31, 100578.

[14] Ahmad, M. A., Eusoff, M. A., Oladoye, P. O., Adegoke, K. A. & Bello, O. S. (2021). Optimization and batch studies on adsorption of Methylene blue dye using pomegranate fruit peel based adsorbent. *Chemical Data Collections*. 32, 100676.

[15] Aziz, A., Hassan, H., Yahaya, N. K. E., Karim, J. & Ahmad, M. A. (2021) Methylene blue dye removal using *Parkia speciosa* pod based activated carbon. *IOP Conference Series: Earth and Environmental Science*. 765(1), 012104.

[16] Mohamad Yusop, M. F., Nasehir Khan, M. N., Zakaria, R., Abdullah, A. Z. & Ahmad, M. A. (2023). Mass transfer simulation on remazol brilliant blue R dye adsorption by optimized teak wood Based activated carbon. *Arabian Journal of Chemistry*. 16(6), 104780.

[17] Ahmad, M. A., Eusoff, M. A., Oladoye, P. O., Adegoke, K. A. & Bello, O. S. (2020). Statistical optimization of Remazol Brilliant Blue R dye adsorption onto activated carbon prepared from pomegranate fruit peel. *Chemical Data Collections*. 28, 100426.

[18] Jawad, A. H. & Surip, S. N. (2022). Upgrading low rank coal into mesoporous activated carbon via microwave process for methylene blue dye adsorption: Box Behnken Design and mechanism study. *Diamond and Related Materials*. 127, 109199.

[19] Khayyun, T. S. & Mseer, A. H. (2019). Comparison of the experimental results with the Langmuir and Freundlich models for copper removal on limestone adsorbent. *Applied Water Science*. 9(8), 170.

[20] Ahmad, M. A., Eusoff, M. A., Oladoye, P. O., Adegoke, K. A. & Bello, O. S. (2021). Optimization and batch studies on adsorption of Methylene blue dye using pomegranate fruit peel based adsorbent. *Chemical Data Collections*. 32, 100676.